



Heriot-Watt University  
Research Gateway

## Fluxing as a new tool for bitumen rheological characterization and the use of time-concentration shift factor (ac)

### Citation for published version:

Zoorob, SE, Mturi, GA, Sangiorgi, C, Dinis-Almeida, M & Habib, NZ 2018, 'Fluxing as a new tool for bitumen rheological characterization and the use of time-concentration shift factor (ac)', *Construction and Building Materials*, vol. 158, pp. 691–699. <https://doi.org/10.1016/j.conbuildmat.2017.10.020>

### Digital Object Identifier (DOI):

[10.1016/j.conbuildmat.2017.10.020](https://doi.org/10.1016/j.conbuildmat.2017.10.020)

### Link:

[Link to publication record in Heriot-Watt Research Portal](#)

### Document Version:

Peer reviewed version

### Published In:

Construction and Building Materials

### General rights

Copyright for the publications made accessible via Heriot-Watt Research Portal is retained by the author(s) and / or other copyright owners and it is a condition of accessing these publications that users recognise and abide by the legal requirements associated with these rights.

### Take down policy

Heriot-Watt University has made every reasonable effort to ensure that the content in Heriot-Watt Research Portal complies with UK legislation. If you believe that the public display of this file breaches copyright please contact [open.access@hw.ac.uk](mailto:open.access@hw.ac.uk) providing details, and we will remove access to the work immediately and investigate your claim.

1 **Fluxing as a New Tool for Bitumen Rheological Characterization and the Use**  
2 **of Time-Concentration Shift Factor ( $a_c$ )**

3 Salah E. ZOOROB<sup>a</sup>, Georges A. MTURI<sup>b</sup>, Cesare SANGIORGI<sup>c</sup>, Marisa DINIS-ALMEIDA<sup>d</sup>  
4 Noor Zainab HABIB<sup>e\*</sup>

5 <sup>a</sup> *Construction and Building Materials Program, Kuwait Institute for Scientific Research, P.O.*  
6 *Box 24885 Safat, 13109 Kuwait. ([szoorob@kISR.edu.kw](mailto:szoorob@kISR.edu.kw))*

7 <sup>b</sup> *CSIR Built Environment, Transport Infrastructure Engineering, PO Box 395, Pretoria 0001,*  
8 *South Africa. ([GMturi@csir.co.za](mailto:GMturi@csir.co.za))*

9 <sup>c</sup> *DICAM-Roads, Dept. of Civil, Environmental and Materials Engineering, University of*  
10 *Bologna, V.le Risorgimento 2, 40136 Bologna, Italy. ([cesare.sangiorgi4@unibo.it](mailto:cesare.sangiorgi4@unibo.it))*

11 <sup>d</sup> *C-MADE, Centre of Materials and Building Technologies, University of Beira Interior,*  
12 *Calçada Fonte do Lameiro, Edifício II das Engenharias, 6200-001 Covilhã, Portugal.*  
13 *([marisa.dinis@ubi.pt](mailto:marisa.dinis@ubi.pt))*

14 <sup>e</sup> *Institute of Infrastructure and Environment, Heriot- Watt University Dubai Campus, P.O.Box*  
15 *294345 Dubai, UAE. ([n.habib@hw.ac.uk](mailto:n.habib@hw.ac.uk))*

16 \*Email: [n.habib@hw.ac.uk](mailto:n.habib@hw.ac.uk)

17 **ABSTRACT**

18 The concept of temperature shift factor ( $a_T$ ) as defined by Doolittle, relating the free volume of a  
19 viscoelastic material at the current and reference states is briefly examined together with the  
20 resultant William-Landel-Ferry equation. This paper highlights the fact that change in free volume  
21 arise not only from temperature variations but can also result from the absorption of solvents and

22 thus a generalized Doolittle relation may also be applied to a solvent concentration shift factor ( $a_c$ ).  
23 To validate this concept, a **small scale** laboratory investigation was carried out by blending 40/60  
24 penetration grade bitumen with various proportions of **one type of** cooking oil and conducting  
25 dynamic shear rheometer frequency sweeps at a range of temperatures. By applying time-  
26 concentration superposition to each flux content, it was possible to shift horizontally ( $a_c$ ) each set  
27 of complex modulus data measured at each test temperature, so that all sets superimpose onto the  
28 master curve of the base bitumen at a preselected reference temperature. A direct relationship  
29 between **conventional** time-temperature shift and **the proposed** time-concentration shift factors **was**  
30 **thus demonstrated using a sample of penetration grade bitumen and one type of vegetable oil.**  
31 **Further experimentation with other bitumen-flux combinations is necessary prior to**  
32 **recommending general adoption of the proposed tool.**

33

34 **Keywords:** Bitumen Rheological Characterization, Time-Temperature Superposition, Time-  
35 Concentration Superposition, Bitumen Fluxing, Free Volume Shifting.

36

## 37 **1. Introduction**

### 38 *1.1 Background of Study*

#### 39 *1.1.1 Introduction to Bitumen Fluxing*

40

41 It is widely accepted that bitumens are miscible with each other to form homogeneous blends in  
42 all proportions, though care must be exercised when blending a penetration grade bitumen with a  
43 blown (oxidised) bitumen. Bitumens can also be blended with a wide variety of crude oil-based  
44 fractions depending on the application. Volatile light fractions (e.g. white spirit) are used when

45 rapid curing is required; less volatile fractions (e.g. kerosene) are used for longer drying times as  
46 for cutback bitumens [Hunter et al., 2015].

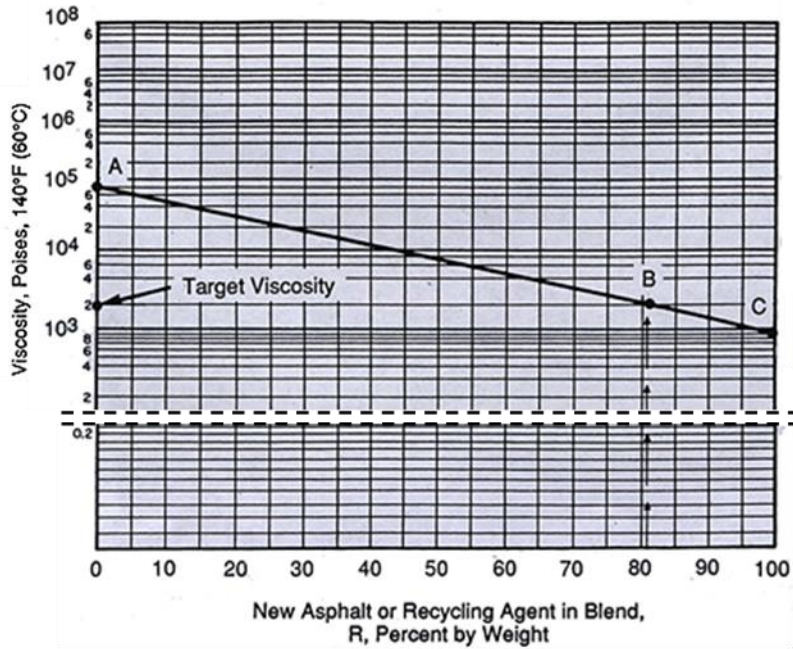
47

48 Bitumen preparations where the viscosity of the binder has been reduced by the addition of  
49 relatively non-volatile oils are referred to as fluxed bitumens. The added oil is known as a fluxing  
50 agent (or fluxant) that is typically gas oil, vegetable based oils [Bailey, 2012] [Eurobitume, 2017],  
51 or methyl esters of fatty acids [Gawel et al., 2010], [Krol et al., 2017].

52

53 When designing reclaimed asphalt pavement (RAP) mixes, it is popular to utilize bitumen blending  
54 charts similar to that shown in Figure 1, [U.S. DoT, 2015] [ASTM D4887]. The viscosity of the  
55 aged bitumen in the RAP is plotted on the left hand vertical scale (Point A). A vertical line  
56 representing the percentage of new bitumen required (R) is drawn and its intersection (Point B)  
57 with the horizontal line representing the target viscosity is determined. A straight line from Point  
58 A, through Point B is next extended to intersect the right hand scale. Point C is the viscosity of the  
59 new bitumen (and/or recycling agent) required to blend with the bitumen in the RAP to obtain the  
60 target viscosity in the blend. Note that the y axis in Figure 1 is a double log scale (Walther  
61 function), thus resulting in an accuracy level which may be described as “approximate”. More  
62 recent work on rejuvenating RAP using bio-materials can also be found in [\[Barco-Carrion, 2017\]](#).

63



64

65 **Fig.1:** Bitumen blending chart [U.S. DoT, 2015]

66

67 There is abundant evidence and theoretical justification in the polymer science literature  
 68 highlighting the fact that when a polymer is diluted (fluxed) with a solvent with which it forms a  
 69 true solution, the viscosity of the blend is reduced [Ferry, 1980]. The primary objective of this  
 70 paper is to simply demonstrate the feasibility of transferring both the theoretical arguments and  
 71 interpretation techniques from fluxing polymers across to the bitumen field. In the following  
 72 sections the theoretical background and justification is first introduced followed by a limited  
 73 experimental proof of concept utilizing a single type of bitumen fluxed with one type of vegetable  
 74 oil.

75

76 *1.1.2 Models for Blended Binders*

77

78 A number of relationships exist for estimating the penetration and softening point of a bitumen  
79 blend. As an example, the Shell Bitumen Handbook recommends the following two formulae  
80 [Hunter et al., 2015]:

$$81 \quad \log P = \frac{A \log P_a + B \log P_b}{100} \quad (1)$$

82 Where: P = penetration of the final blend, P<sub>a</sub> = penetration of component 'a', P<sub>b</sub> = penetration of  
83 component 'b', A = % of component 'a' in the blend, B = % of component 'b' in the blend.

$$84 \quad S = \frac{A S_a + B S_b}{100} \quad (2)$$

85 Where: S = softening point of the final blend, S<sub>a</sub> = the softening point of component 'a', S<sub>b</sub> =  
86 softening point of component 'b', A = % of component 'a' in the blend, B = % of component 'b'  
87 in the blend.

88 It is interesting to note that equation 1 is likely derived from early work conducted by Arrhenius  
89 to predict the [steady state](#) viscosity ( $\eta_0$ ) of ideal binary mixtures of mineral oils [Briant et al.,  
90 1989]:

$$91 \quad \ln \eta_0 = \frac{V_1}{V} \ln \eta_1 + \frac{V_2}{V} \ln \eta_2 \quad (3)$$

92 Where:  $\eta_1$  and  $\eta_2$  = the viscosities of the component oils, V<sub>1</sub> and V<sub>2</sub> = volumes of the oils making  
93 up the blend, V = volume of the blend.

94

95 Another method worthy of mentioning is the Refutas viscosity blending function which was  
96 developed to predict blend viscosities of all petroleum components from gasoline to vacuum  
97 residue [Barabas et al., 2011]. In this method a Viscosity Blending Index (VBI) of each component  
98 is first calculated and then used to determine the VBI of the liquid mixture as shown below.

99 
$$VBI_i = 14.534 \times \ln(\ln(v_i + 0.8)) + 10.975 \quad (4)$$

100 Where:  $v_i$  = kinematic viscosity in centistokes (cSt). It is important that the kinematic viscosity of  
 101 each component of the blend be obtained at the same temperature.

102

103 The VBI of the liquid mixture is then calculated as follows:

104 
$$VBI_{mixture} = \sum_{i=1}^N (x_i \times VBI_i) \quad (5)$$

105 Where:  $x_i$  = the mass fraction of component “i” of the blend; N = the number of components.

106

107 The kinematic viscosity of the mixture can then be estimated using the viscosity blending number  
 108 of the mixture using the equation below.

109 
$$v_{mixture} = \exp\left(\exp\left(\frac{VBI_{mixture} - 10.975}{14.534}\right)\right) - 0.8 \quad (6)$$

110 Soleymani et al. (1999) conducted a thorough review and investigation on bitumen blending. The  
 111 change in complex shear modulus ( $G^*$ ) of various blends of laboratory aged and unaged binders,  
 112 also blended with various proportions of recycling agents were studied at high and intermediate  
 113 pavement temperatures with a Dynamic Shear Rheometer (DSR). The study demonstrated that  
 114 linear relationships for shear modulus ( $G^*$ ) of the blended binders can be represented numerically  
 115 as follows:

116 
$$\text{Log } G_{Blend}^* = \text{Log } G_{Aged}^* - X \cdot \text{Log} \left( \frac{G_{Aged}^*}{G_{Recycling Agent}^*} \right) \quad (7)$$

117 Where: X = proportion of recycling agent by total weight in the blend.

118

119 *1.2 Background to the Free Volume Model and the WLF Equation*

120 The free volume model is based on the assumption that the mechanical response of a viscoelastic  
121 polymer is dependent on the ability of its molecular chains to accommodate applied deformations.  
122 Free volume may be visualized as the volume that is not occupied by the molecular chains in a  
123 material that can be considered an indicator of molecular segmental mobility, where greater free  
124 volume provides the extra mobility needed to accommodate applied deformations rapidly. [Roy,  
125 2001]

126 According to the free volume theory, the glass transition temperature ( $T_g$ ) represents the  
127 temperature that polymers have a certain universal free volume which controls the molecular  
128 mobility. In polymer science,  $T_g$  is also described as the point, or narrow region, on the temperature  
129 scale where the thermal expansion coefficient undergoes a discontinuity and below which the  
130 configurational rearrangements of polymer chain backbones are extremely slow [Ferry, 1980].

131 The internal mobility of the system (expressed as viscosity) can be related to the fractional free  
132 volume empirically by the Doolittle viscosity equation 8. Equation 8 then provides the starting  
133 point to derive the William-Landel-Ferry (WLF) equation from the free volume theory [Gedde,  
134 2013].

135 
$$\eta = A \cdot \exp\left(\frac{B}{f}\right) \tag{8}$$

136 Where:  $\eta$  = viscosity, A and B are constants, and f is the fractional free volume.

137 Doolittle defined a temperature shift factor ( $a_T$ ) relating the free volume of a material at the current  
138 and reference states through the expression:

139 
$$a_T = \frac{\exp\left(\frac{B}{f}\right)}{\exp\left(\frac{B}{f_r}\right)} = \exp\left(B \left(\frac{1}{f} - \frac{1}{f_r}\right)\right) \tag{9}$$



140 Where:  $f$  = fractional free volume at temperature  $T$ , and  $f_r$  = the fractional free volume at the  
 141 reference temperature  $T_r$ .

142

143 The fractional free volume at temperature  $T$  can be expressed as:

$$144 \quad f = f_r + \alpha_f(T - T_r) \quad (10)$$

145 Where:  $\alpha_f$  = the coefficient of expansion of the fractional free volume. Insertion of equation 10  
 146 into equation 9 gives:

$$147 \quad a_T = \exp\left(B\left(\frac{1}{f_r + \alpha_f(T - T_r)} - \frac{1}{f_r}\right)\right) = \exp\left(B\left(\frac{-\alpha_f(T - T_r)}{f_r(f_r + \alpha_f(T - T_r))}\right)\right)$$

$$148 \quad = \exp\left(-\frac{B}{f_r}\left(\frac{\alpha_f(T - T_r)}{f_r + \alpha_f(T - T_r)}\right)\right) = \exp\left(\frac{\left[\frac{-B}{f_r}\right](T - T_r)}{\left[\frac{f_r}{\alpha_f}\right] + (T - T_r)}\right) \quad (11)$$

149 The following expression can be obtained by taking the logarithm of equation 11 [Gedde, 2013]:

$$150 \quad \log a_T = \frac{\left[\frac{-B}{2.303f_r}\right](T - T_r)}{\left[\frac{f_r}{\alpha_f}\right] + (T - T_r)} \quad (12)$$

151

152 The WLF equation, expressed in general terms has the following form:

$$153 \quad \log a_T = \frac{-C_1(T - T_r)}{C_2 + (T - T_r)} \quad (13)$$

154 Where:  $a_T = \eta_T/\eta_{T_r} = \tau_T/\tau_{T_r}$ , ( $\eta$  represents the viscosity and  $\tau$  represents a characteristic segmental  
 155 relaxation time at temperatures  $T$  and  $T_r$ ,  $C_1$  and  $C_2$  are constants). When the reference temperature

156  $T_r$  is set equal to the glass transition temperature ( $T_g$ ),  $C_1$  and  $C_2$  have been found to be almost  
157 universal constants for a wide range of polymers ( $C_1 = -17.44$  and  $C_2 = 51.6$  K).

158

159 The WLF can equally be rewritten in natural log terms:

$$160 \frac{-1}{\ln(a_T)} = \frac{C_2 + (T - T_r)}{C_1(T - T_r)} = \frac{C_2}{C_1(T - T_r)} + \frac{1}{C_1} \quad (14)$$

161 The WLF can also be rearranged to obtain the universal constants  $C_1$  and  $C_2$  from a linear graphical  
162 plot as follows:

$$163 \frac{(T - T_r)}{\log a_T} = \frac{-(T - T_r)}{C_1} - \frac{C_2}{C_1} \quad (15)$$

164

### 165 *1.3 Introducing the Generalized Shift Factor*

166 The free volume change of viscoelastic polymers has been typically associated with thermal  
167 changes and resulted in the time-temperature trade-off during material characterization. However,  
168 this change in free volume can also arise from solvent absorption and/or from mechanical stress  
169 as studied through the influence of pressure on the glass transition temperature [Emri, 1986].

170 It has thus been argued that temperature, solvent (or plasticizer or flux) concentration and  
171 mechanical dilation all influence the time scale, and hence the fractional free volume, of the  
172 material in a similar manner. The fractional free volume can be expressed as [Roy, 2001]:

$$173 f = f_0 + A.\alpha(t).dT + B.M(t).\sigma_{kk} + C.\gamma(t).dc \quad (16)$$

174 Where;  $f_0 =$  the fractional free volume at an arbitrary reference temperature  $T_0$ ,  $\alpha(t)$  and  $\gamma(t)$  are  
175 the volume coefficients of thermal and solvent expansion respectively. In general,  $\alpha(t)$  and  $\gamma(t)$  are

176 functions of temperature (T), solvent concentration (c), the creep compliance M(t) is a function  
 177 of mechanical dilation  $\theta(t)$ ,  $\sigma_{kk}$  is the first stress invariant, and A, B, C are constants to be  
 178 determined.

179  
 180 For small changes in variables below the glass transition temperature of the polymer and the  
 181 boiling point of the penetrant, it may be assumed that  $\alpha(t)$ ,  $\gamma(t)$  and M(t) are constants with respect  
 182 to time. Under such conditions, equation 16 can be reduced to [Roy, 2001]:

$$183 \quad f = f_0 + \alpha\Delta T + \gamma\Delta c + \delta\theta \quad (17)$$

184 Where:  $\theta = \epsilon_{kk}$  the first strain invariant, and  $\delta$  is a material constant.

185  
 186 Hence the shift factor  $a(T,c,\theta)$  can be expressed as a function of temperature (T), solvent  
 187 concentration (c) and mechanical dilation ( $\theta$ ). Substituting equation 17 into equation 9 gives the  
 188 nonlinear shift factor [Roy, 2001]:

$$189 \quad \text{Log } a(T, c, \theta) = - \frac{B}{2.303f_0} \frac{\alpha \Delta T + \gamma \Delta c + \delta \theta}{f_0 + \alpha \Delta T + \gamma \Delta c + \delta \theta} \quad (18)$$

190 For negligible solvent concentrations and dilation, equation 18 reduces to the WLF equations (13  
 191 or 14).

192  
 193 There is also a correction that may be applied in the vertical direction (i.e. parallel to the y axis)  
 194 along with the shift in the x axis. The temperature-dependent, vertical shift factor  $b_T$  is usually  
 195 defined as the ratio of stress determined at temperature T to a “reduced stress” that is the value at  
 196 a “reference temperature”  $T_0$ . The assumption that stress magnitudes, e.g. G(t),  $G'(\omega)$  and  $G''(\omega)$ ,

197 are proportional to the product of the density and temperature implies that the vertical shift factor  
198  $b_T(T)$  has the following form [Schausberger A., 1995]:

$$199 \quad b_T = (T_o \times \rho_o) / (T \times \rho) \quad (19)$$

200 This vertical correction is invalid for the glassy state and can only be made for the rubbery state  
201 (above  $T_g$ ). The value of  $b_T$  is normally close to unity as the dependence of sample density on  
202 temperature is relatively small.

203

#### 204 *1.4 Justifying the use of use of Concentration Shift Factor $a_c$*

205 In this section we will ignore the effects of temperature and mechanical dilation and focus on the  
206 influence of adding a non-volatile solvent (or flux or plasticizer) to our binder at constant  
207 temperature and assuming no dilation effects.

208

209 A generalized Doolittle relation can thus be applied to the concentration shift factor ( $a_c$ ) as follows  
210 [Schausberger A., 1995].

211 It is worth noting that equation 20 is comparable to equation 9.

$$212 \quad a_c = \exp\left(D \left(\frac{1}{f} - \frac{1}{f_r}\right)\right) \quad (20)$$

213 Where:  $f$  = fraction of free volume of the plasticized binder,  $f_r$  = fraction of free volume of the pure  
214 binder. The parameter  $D$  is assumed to be independent of molar mass, temperature and  
215 concentration. The parameter  $f$  is defined below (comparable to equation 10)

$$216 \quad f = f_r + \beta w_1 \quad (21)$$

217 Where:  $w_1$  = the weight fraction of the additive,  $\beta$  = the pertinent parameter relating free volume  
218 to weight fraction of additive. The parameter  $\beta$  is in essence a measure of the molar plasticizing  
219 activity of an additive.

220 Further manipulation of the equations 20 and 21 yields the following equation [Schausberger A.,  
221 1995].

$$222 \quad \frac{-1}{\ln a_c} = \frac{f_r}{D} + \left[ \frac{f_r^2}{D\beta} \times \frac{1}{w_1} \right] = \frac{C_{22}}{C_{11}(w_1)} + \frac{1}{C_{11}} \quad (22)$$

223 Equation 22 is essentially comparable to equation 14, where  $a_T$  is equivalent to  $a_c$ ,  $(T_r - T)$  is  
224 equivalent to  $w_1$ ,  $C_1$  is equivalent to  $C_{11}$  and  $C_2$  is equivalent to  $C_{22}$ . Equation 22 can also be  
225 rearranged and expressed in a similar manner to equation 15 as follows:

$$226 \quad \frac{w_1}{\log a_c} = \frac{-w_1}{C_{11}} - \frac{C_{22}}{C_{11}} \quad (23)$$

227

228

229

## 230 **2. Materials and Testing Methods**

231 In this investigation, a sample of Shell 40/60 penetration grade bitumen (pen. = 56 dmm, S.P. =  
232 50.4°C) (Kuwaiti crude) was blended with vegetable oil to produce a range of bitumen/oil blends.

233 Groundnut (also known as Peanut) cooking oil, readily available from most supermarkets in the

234 UK, was arbitrarily selected and used in this investigation. [Typical groundnut oil characteristics](#)

235 [based on extensive literature by \[Tan, 2001\] and \[O'Brien, 2004\] are as follows: Fatty Acid](#)

236 [content = 0.05 %, Iodine Value = 95.23 \(g of I<sub>2</sub>/100g of oil\), Peroxide value = 6.82 \(meg/kg oil\),](#)

237 [and Anisidine value = 5.22. Typical fatty acid distribution is as follows: Saturated fatty acid](#)

238 (mainly Palmitic and Stearic acid) = 22.5%, Mono-unsaturated fatty acid (primarily Oleic acid) =  
239 50.1%, Poly-unsaturated acid (primarily Linolenic acid) = 27.4%.

240

241 In the first part of the investigation, bitumen/oil blends were produced one blend at a time. The  
242 production sequence started by heating the 40/60 penetration grade to a temperature of 160°C in  
243 an oven, transferring the bitumen tin on to a hot plate, and adding the required amount of preheated  
244 vegetable oil whilst continuously stirring each blend manually for 10 minutes using a kitchen  
245 whisker. To minimize the extent of vegetable oil oxidation, for each blend, approximately 0.5 L  
246 of oil was placed in a capped small glass bottle in a preheated oven set at 160°C for 30 minutes  
247 and a fresh sample of oil was used for each blend. Six samples of bitumen/oil blends were produced  
248 at 0, 2, 4, 6, 8 and 10% oil contents by mass. As expected, the vegetable oil blended readily with  
249 the bitumen and there was a noticeable increase in fluidity/workability as the oil content was  
250 increased.

251

252 The 40/60 penetration grade and the various blends were also subjected consecutively to the rolling  
253 thin film oven test (RTFOT) [ASTM D2872] and pressure ageing vessel (PAV at 110°C) [ASTM  
254 D6521] laboratory ageing protocols. For every blend at each ageing condition, i.e. Virgin, RTFOT,  
255 RTFOR+PAV, dynamic shear rheometer (DSR) test samples were cast into (8mm and 25mm  
256 diameter) silicon moulds (3 samples each size).

257 Oscillatory tests were undertaken by means of a Malvern Kinexus model DSR in strain control  
258 mode of loading using parallel plate geometry in accordance with AASHTO T315. The  
259 temperature range from 0 to 40°C (in steps of 5°C) was investigated using an 8mm diameter plate

260 (2mm gap), whilst the range from 45 to 75°C (in steps of 5°C) was investigated using a 25mm  
261 diameter plate (1mm gap). Strain sweeps were initially conducted (results not shown in this paper)  
262 to establish the linear viscoelastic limits for base bitumen at the various test temperatures.  
263 Subsequently, at each test temperature, a frequency sweep was conducted (0.1 to 10 Hz) at a strain  
264 amplitude of 0.5%, well within the linear viscoelastic limit of the hardest sample tested in this  
265 investigation.

266

### 267 3. Results and Discussion

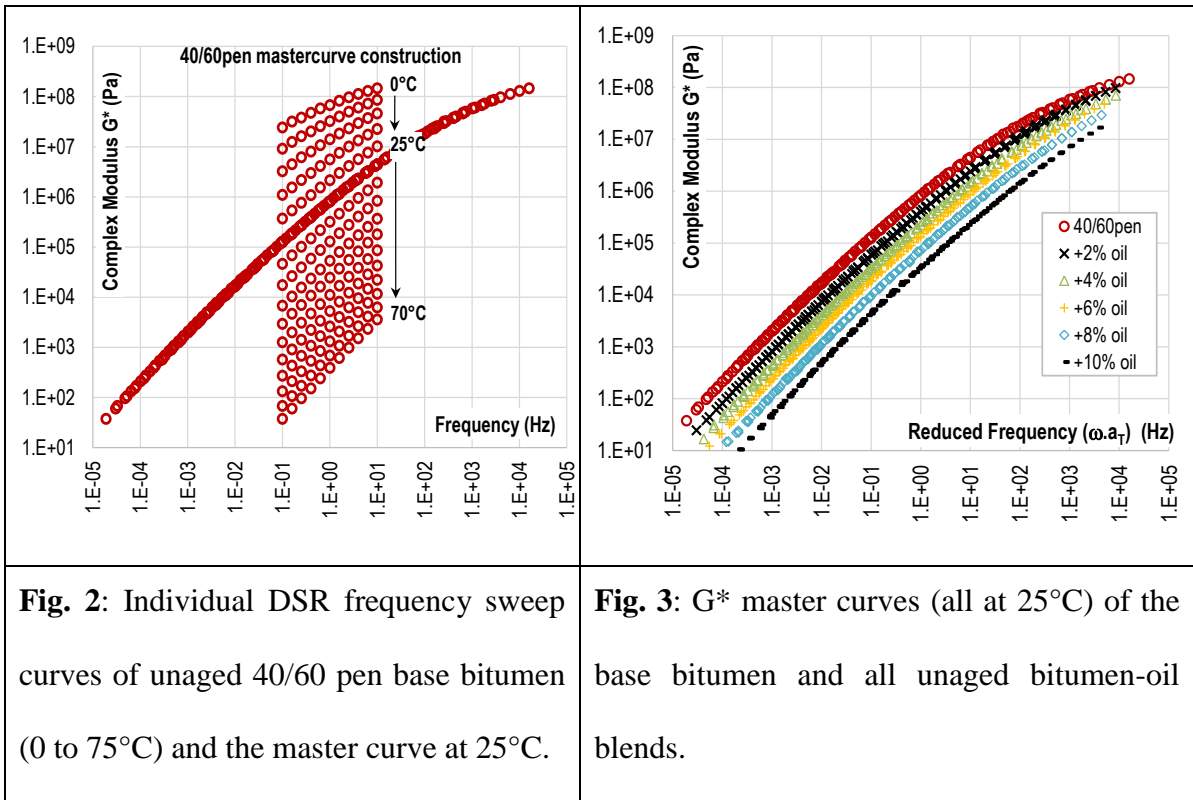
268 Figure 2 shows complex modulus ( $G^*$ ) versus frequency (0.1-10 Hz) individual curves obtained  
269 from DSR frequency sweeps of the 40/60 penetration grade bitumen at each test temperature (0 to  
270 75°C). Also presented is the master curve obtained by shifting the individual iso-thermal curves  
271 across the frequency axis, using the time-temperature superposition (TTS) principle, to a reference  
272 temperature  $T_r$  of 25°C. The combined  $G^*$  master curve thus extends over a much wider frequency  
273 range. TTS analysis and the generation of shift factors was carried out on the raw DSR data with  
274 the aid of proprietary software (rSpace™) pre-installed by Malvern on the Kinexus DSR. In  
275 essence the software carries out non-linear regression analysis on the rheological data. A thorough  
276 explanation of the background and comparison of various procedures for TTS, shift factors and  
277 the production of master curves can be found in Chapter 11 of [Ferry, 1980] and [Yusoff et al.,  
278 2011].

279

280 The same TTS procedure was repeated for each bitumen/oil blend and the results of the  $G^*$  master  
281 curves (at a reference temperature of 25°C) are shown in Figure 3. All the  $G^*$  master curves show

282 the characteristic 45° asymptote at low frequencies (high temperatures), and they all tend in a  
 283 smooth transition towards a common limiting stiffness value (glassy  $G^*$ ) at the upper end of the  
 284 frequency (lower temperature) spectrum.

285



286

287 Figure 4 shows the results of the TTS principle having been applied to the phase angle ( $\delta$ ) results  
 288 to generate  $\delta$  master curves also at 25°C. Observing either Figure 3 or Figure 4, one notices that  
 289 the  $G^*$  or  $\delta$  master curves of the various blends have high resemblance with respect to shape and  
 290 presented merely simple horizontal shifts (translations) of the 40/60pen master curve across the  
 291 frequency axis. Simple visual interpretation of the  $G^*$  or  $\delta$  master curves indicates that vegetable  
 292 oil blending has not introduced any visibly obvious rheologic modifications to the base bitumen  
 293 (e.g. major changes in slope, curvature, or discontinuities) beyond what is expected from a



294 chemically compatible non-interactive flux (i.e. simple reduction in viscosity), [though this requires](#)  
 295 [further quantitative verification with the aid of optimization techniques.](#)

296

297 To emphasise the point that the various binder curves are merely horizontal translations, Figure 5  
 298 shows the 10% oil blend  $G^*$  master curve superimposed on the control 40/60pen  $G^*$  master curve  
 299 (all at 25°C), and the two curves in Figure 5 are almost inseparable.

300

301

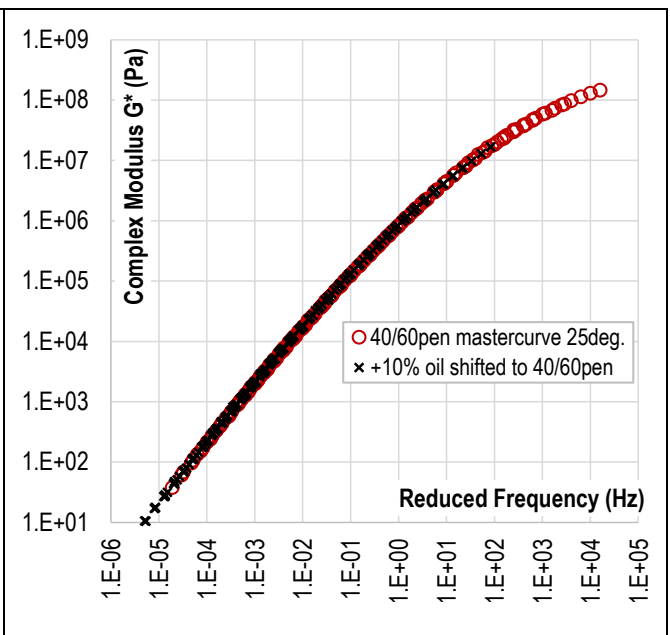
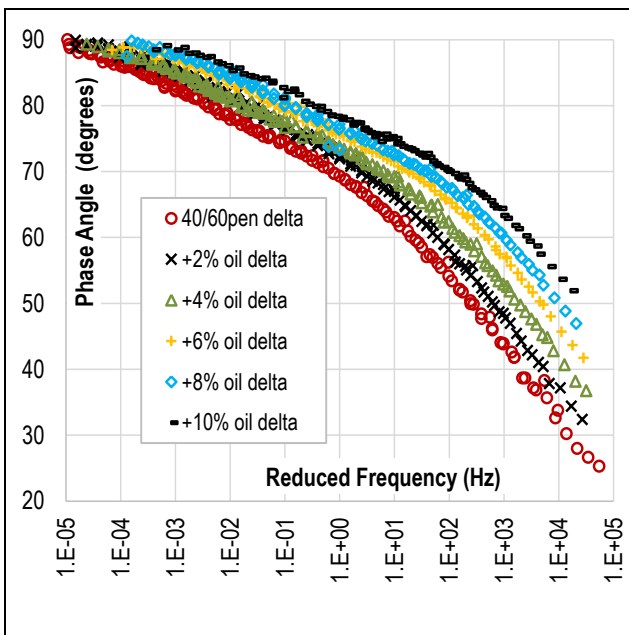


**Fig. 4:** Phase angle ( $\delta$ ) master curves (25°C) of the unaged base bitumen and bitumen-oil blends.

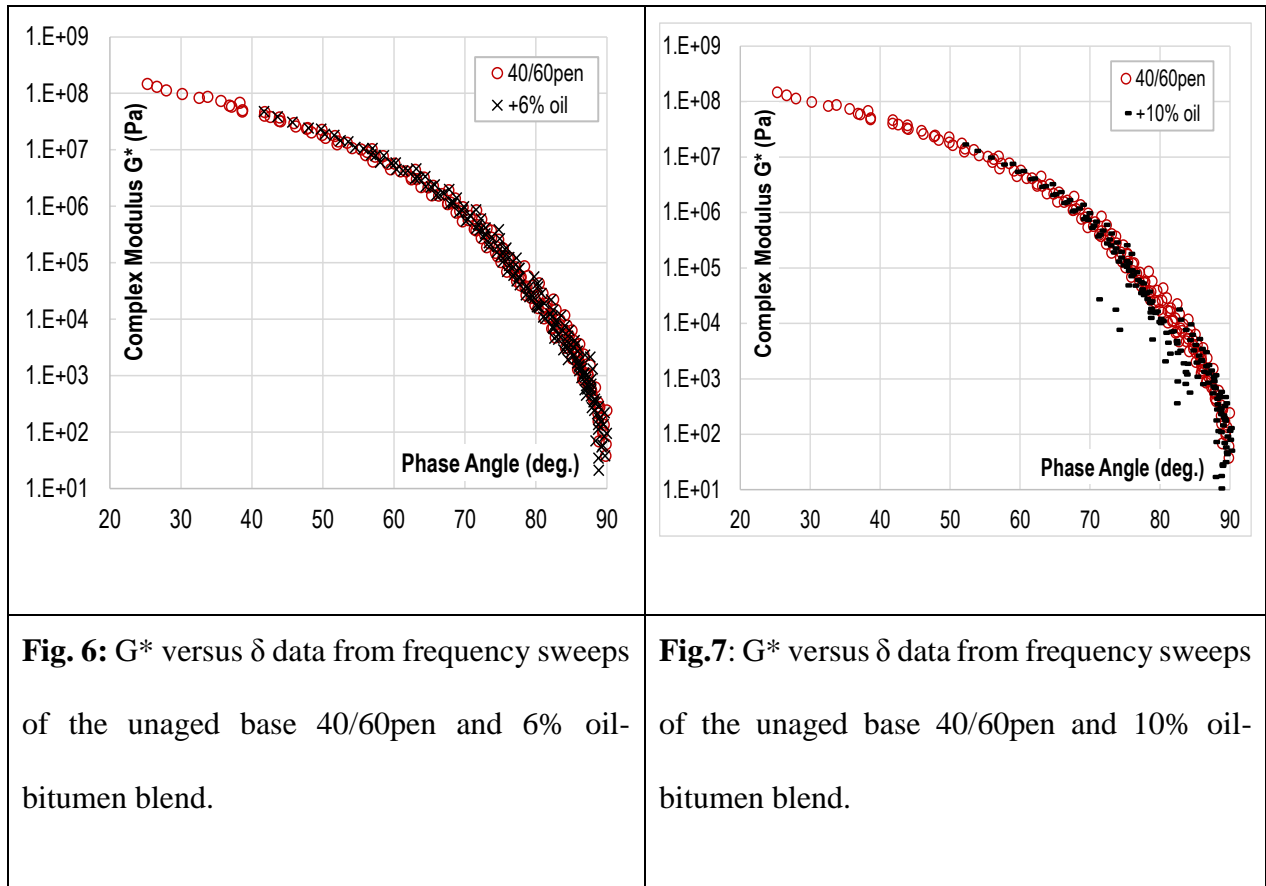
**Fig. 5:**  $G^*$  master curve of the unaged 10% oil-bitumen blend superimposed onto the unaged base 40/60pen  $G^*$  master curve at 25°C.

302

303 In Figure 6, the relationship between  $G^*$  and  $\delta$  over the entire temperature and frequency range  
304 are presented in the form of Black diagram curves for two binder types, i.e. the base 40/60pen  
305 bitumen and the 6% oil-bitumen blend. The advantage of plotting Black diagrams is that for each  
306 binder type, the raw  $G^*$  and  $\delta$  data at all test temperatures can be simply visualized in their original  
307 (un-shifted) form. [Simple visual observation shows](#) that the 6% oil blend (un-shifted frequency  
308 sweep data) superimposes on the thermo-rheologically simple 40/60pen base bitumen curve with  
309 a [reasonably](#) good fit. Identical behaviour was observed for the 2% and 4% oil blends.

310

311 Beyond 6% oil addition, the assumption of rheological “simplicity” appears to become gradually  
312 less credible. The example shown in Figure 7 is a Black diagram showing the 10% oil blend  
313 superimposed onto the 40/60 pen base bitumen curve. It is clear in Figure 7 that the compatibility  
314 or peptizing ability of the vegetable oil in the bitumen becomes more questionable beyond 6%.  
315 Utilizing black diagrams is a very effective technique to ensure compatibility (absence of phase  
316 separation) of the various blend components. Relying on the goodness of fit of superimposed  
317 (shifted)  $G^*$  curves, as shown earlier in Figure 5 as an example, would not have revealed the [lack](#)  
318 [of](#) compatibility issue at 10% oil content.



319 The potential for superimposing Black diagrams of various binders was also assessed using  
 320 RTOFT+PAV conditioned samples. Figure 8 presents the Black diagrams for the 40/60pen virgin,  
 321 40/60pen aged and 6% oil-bitumen blend/aged binders. As expected, aged binders had lower phase  
 322 angle values (to the left side) of the unaged 40/60pen. [Simple visual observation of the goodness](#)  
 323 of fit of the superimposed 6% oil-bitumen aged blend onto the aged 40/60pen shown in Figure 8  
 324 was not as good as was the case for the virgin binders (Figure 6). This can be attributed to the fact  
 325 that due to the completely different chemical composition, vegetable oils age at a different rate  
 326 compared to petroleum derived bituminous binders. The triacylglycerol structure, which forms the  
 327 backbone of most vegetable oils are associated with different fatty acid chains. The presence of  
 328 unsaturation in the triacylglycerol molecule (e.g. due to C=C from oleic, linoleic, and linolenic  
 329 acid moieties, functions as the active sites for various oxidation reactions [Erhan, 2005] [Krol et

330 al., 2017]. Once again a simple visual assessment shows that the goodness of fit of the Black  
 331 diagrams of the aged binders deteriorates rapidly above 6% oil content.

332

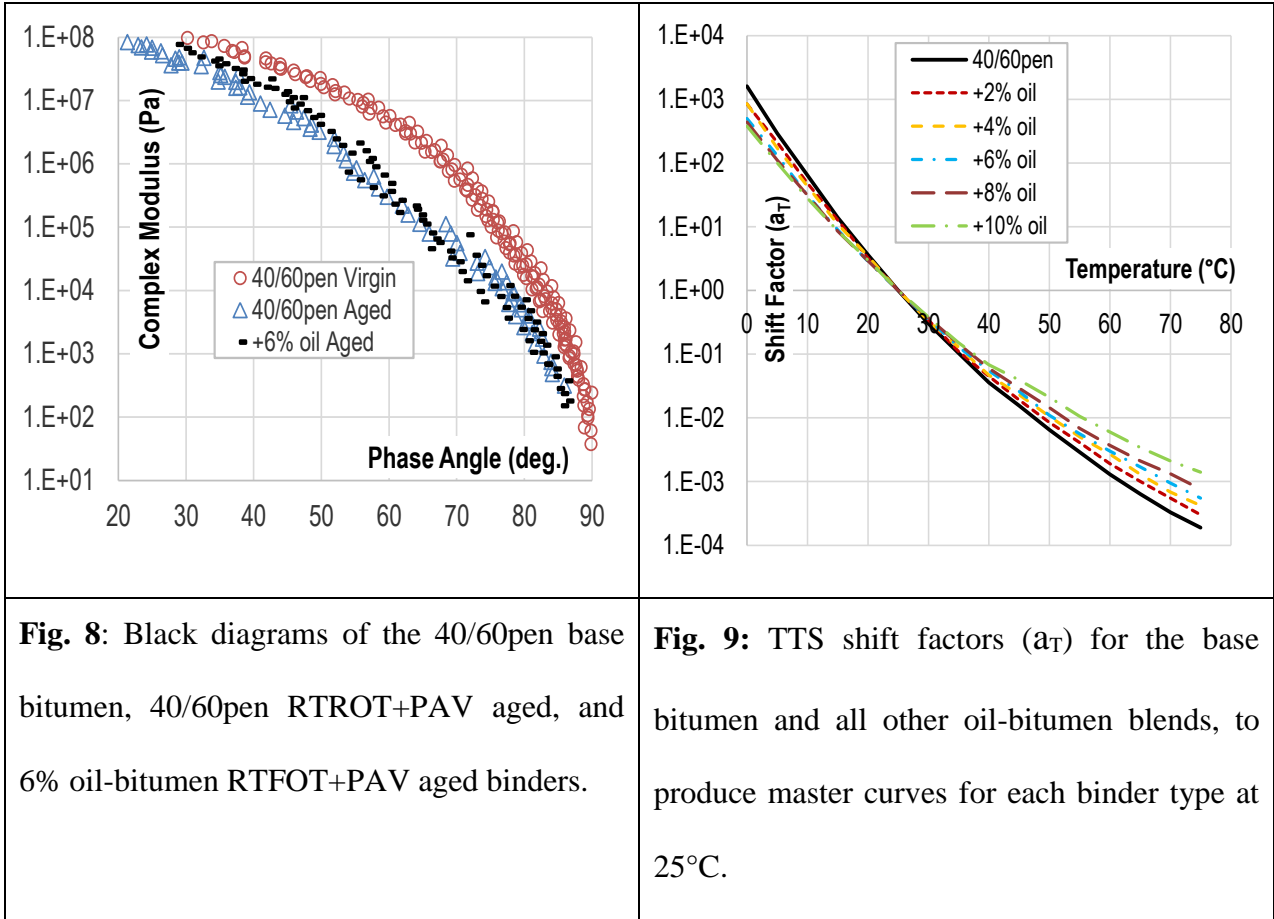


**Fig. 8:** Black diagrams of the 40/60pen base bitumen, 40/60pen RTROT+PAV aged, and 6% oil-bitumen RTFOT+PAV aged binders.

**Fig. 9:** TTS shift factors ( $a_T$ ) for the base bitumen and all other oil-bitumen blends, to produce master curves for each binder type at 25°C.

333

334 Figure 9 presents the time-temperature shift (TTS) factors ( $a_T$ ) for each of the base bitumen and  
 335 the five unaged blends investigated. The  $a_T$  values shown indicate the amount of horizontal shifting  
 336 (across the frequency axis) that must be applied to each binder type at each test temperature to  
 337 generate master curves at 25°C. It is interesting to note that overall, the amount of shifting required  
 338 at any one temperature reduces progressively as the oil content increases (softer binder).

339

340 Each line in Figure 10 is a graphical presentation of the WLF equation 15 for a particular binder  
341 at the reference temperature  $T_r$  of 25°C. The slope of each line is equivalent to  $(-1/C_1)$  and the  
342 intercept with the y axis at  $(T - T_r = 0)$  represents the constant  $(-C_2/C_1)$ . The values of the constants  
343  $C_1$  and  $C_2$  for each binder blend is presented in Table 1. Using these constants, for each binder  
344 type, it would be possible to determine the amount of horizontal shift ( $a_T$ ), across the frequency  
345 axis, required for a set of  $G^*$  data acquired at any test temperature ( $T$ ) to form a master curve of  
346 that binder at the reference temperature ( $T_r$ ) of 25°C.

347

348 Next, using the concept of time-concentration superposition, for each flux content, it is possible to  
349 shift horizontally each of the sets of  $G^*$  data measured at any test temperature, so that all sets  
350 individually superimpose on to the master curve of the 40/60pen base bitumen at 25°C. An  
351 example of the 10% oil raw data and the concentration-shifted data is shown in Figure 11.

352

353

354

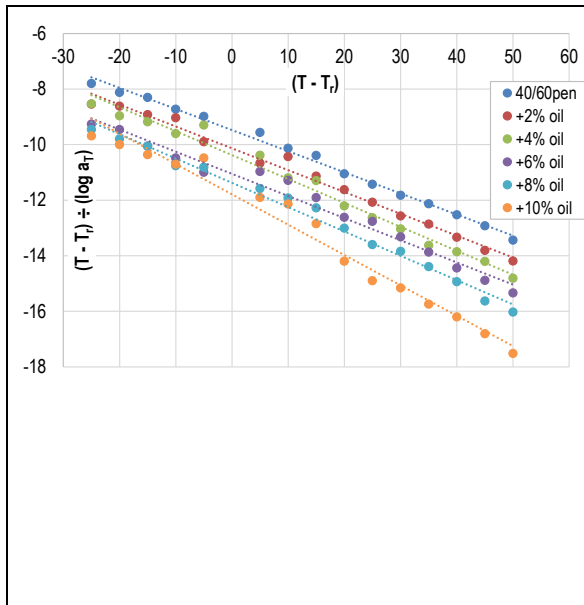


**Fig.10:** Graphical representation of the WLF equation for each of the binders tested in this investigation

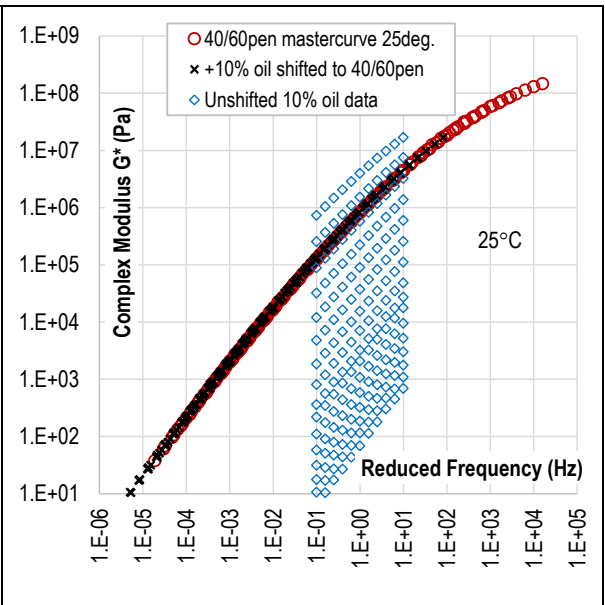


**Fig.11:** A graphical representation of shifting 10% oil-bitumen blend individual frequency sweep curves (obtained at different temperatures) to superimpose on to the 40/60pen base bitumen master curve at 25°C. The amount of shifting required at each temperature represents the concentration shift factors ( $a_c$ ).

355  
356  
357  
358  
359  
360

Binder type	WLF constant $C_1$	WLF constant $C_2$
40/60pen	30.29	124.69
40/60pen + 2% oil	29.29	128.91
40/60pen + 4% oil	26.71	120.34
40/60pen + 6% oil	28.89	138.61
40/60pen + 8% oil	26.28	129.81
40/60pen + 10% oil	21.08	107.93

361 Table 1: Values of the WLF constants  $C_1$  and  $C_2$  for all binder blends investigated (reference  
362 temperature = 25°C).

363

364 Using the analogy of polymer dilution with a solvent, the following corresponding explanations  
365 may be proposed regarding the physical effects of fluxing on bitumens. When a polymer is diluted  
366 with a solvent of low molecular weight, with which it forms a true solution in the sense that the  
367 solvent is molecularly dispersed, the local (monomeric) friction coefficient (i.e. the resistance  
368 encountered by a sub-molecule junction moving through its surroundings) is usually sharply  
369 reduced. Each polymeric chain unit has in its vicinity diluent molecules as well as other polymeric  
370 segments, and the former can be displaced in translatory motion much more easily, thus lowering  
371 the effective local viscosity. With increasing proportion of diluent, the monomeric friction  
372 coefficient is normally diminished, as evidenced by displacement of logarithmic plots of  
373 viscoelastic functions in the transition zone to higher frequencies or shorter times with relatively  
374 little change in shape, which agrees with the limited experimental data presented in this  
375 investigation, [Ferry, 1980] [Rwei, 2014].

376

377 Moreover, the addition of a diluent of low molecular weight depresses  $T_g$  sharply and this  
378 depression can be attributed to the introduction of additional free volume with the diluent, as would  
379 be expected if the fractional free volume of the diluent exceeds that of the polymer and the free  
380 volumes are additive. With increasing dilution of polymers, the temperature dependence of  
381 relaxation times referred to a fixed reference temperature  $T_r$  becomes less pronounced as  $T_g$  is  
382 depressed more and more below  $T_r$  and  $c_2$  increases while  $c_1$  decreases. Furthermore, plasticizing  
383 effectiveness increases rapidly as the temperature is lowered and  $T_g$  is approached causing large  
384 changes in shift factor  $a_c$  [Ferry, 1980].

385

386 The results in table 1 do not show a clear trend of  $C_1$  or  $C_2$  values increasing or otherwise with  
387 amount of fluxing, though it must be reiterated that these results are based on one bitumen grade  
388 in combination with one oil type and more work is needed.

389

390 Figure 12 shows a plot of “ratio of added flux to the log of concentration shift factor ( $a_c$ )” versus  
391 the “proportion of added flux by mass”. Each line in Figure 12 represents a solution of equation  
392 23 (which is comparable to the WLF equation 15) at a specific temperature. For the sake of clarity,  
393 only the results of 25, 30, 35, 40, 45, 50, 55°C are shown.

394

395 As an example, the second line from the top in Figure 12, shows the amount of shifting that has to  
396 be performed across the frequency axis for a range of oil flux contents (all tested at 30°C), to bring  
397 back their individual 30°C  $G^*$  values to the values equivalent to the  $G^*$  of the base 40/60pen  
398 bitumen at the reference temperature of at 25°C. Similarly, the third line represents the amount of



399 shifting that needs to be carried out, if the fluxed binders are all at 35°C, so that the  $G^*$  values are  
400 equivalent to the 40/60pen master curve at 25°C, etc.

401

402 Interestingly, the lines in Figure 12 do not represent linear relationships and hence do not allow  
403 the direct use of equation 23 (by extrapolation to  $w = 0$ ) for deriving the  $C_{11}$  and  $C_{22}$  constants.

404 One possible solution would be to plot the data on a log-log scale as shown in Figure 13, which  
405 would “straighten” the curves. Figure 13 is one potential solution, though the use of log-log scales

406 to artificially produce linear graphical relationships introduces a degree of inaccuracy in the  
407 procedure. There are likely to be better mathematical treatments of shift factors than the WLF

408 equation, for example a modified form of the Kaelble shift equation [Rowe et al., 2011], may allow  
409 direct use of the data shown in Figure 12 without having to resort to double log scales, which is

410 beyond the scope of this [simplified](#) conceptual paper.

411

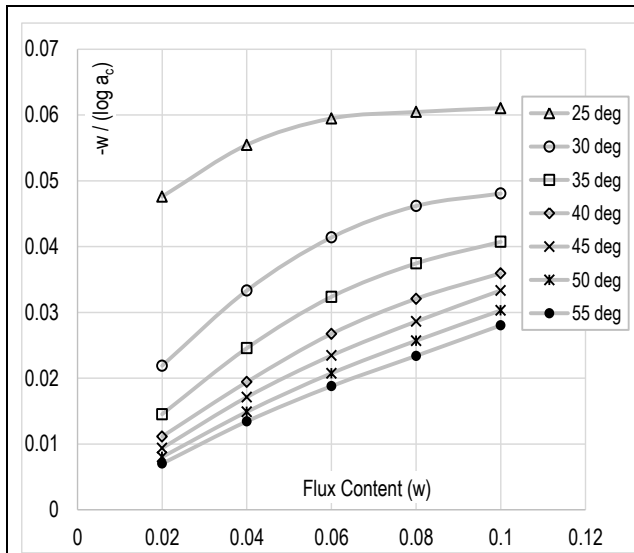


**Fig. 12:** Ratio of added flux by mass to log of concentration shift factors ( $a_c$ ) versus flux content.

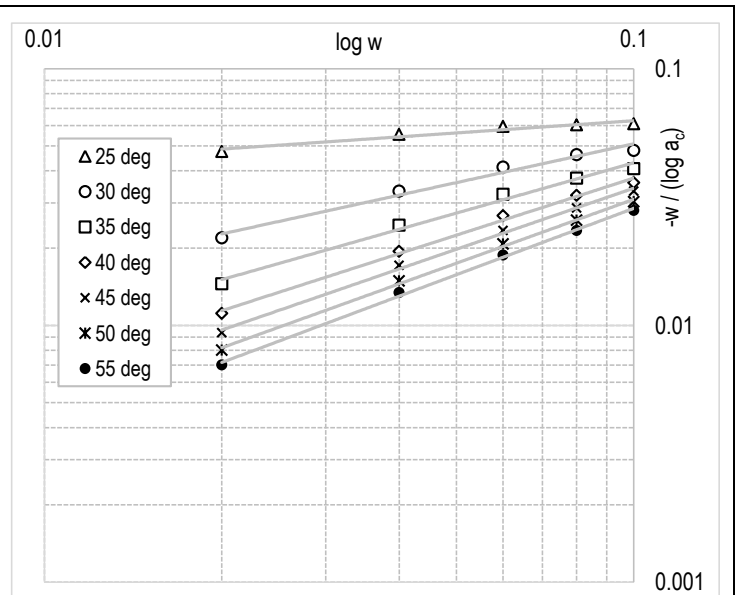


**Fig. 13:** Log-Log plot of the data shown in Figure 12.

412

413 Now going back to the original objective, which is simply attempting to link temperature shift to  
 414 concentration shift. As long as the TTS relationships (equation 15) are available for a particular  
 415 binder grade, and that concentration shift data ( $a_c$ ) can be produced accurately for a range of flux  
 416 concentrations and a range of test temperatures, it should be possible to use the raw data directly  
 417 to produce simple concentration shift charts.

418

419 Figure 14 shows a number of  $a_c$  lines (dashed curves) versus test temperature. Each curve  
 420 represents data for one flux content and all the curves shown in the Figure can be readily fitted

421 using power law relationships of the form;  $a_T = aT^b$  (where  $a$  and  $b$  are constants and  $T =$   
422 temperature) all having  $R^2$  values in excess of 0.99.

423

424 The solid horizontal “red” line represents an example of a temperature shift factor ( $a_T = 0.0065$ )  
425 for the 40/60pen to a temperature  $T = 50^\circ\text{C}$  from a reference temperature  $T_r = 25^\circ\text{C}$ . By equating  
426  $a_T$  to  $a_c$ , we can read off from the intercept of the horizontal line with each  $a_c$  curve, the amount  
427 of flux and the test temperature that would be equal to a temperature rise of  $25^\circ\text{C}$  (i.e. from 25 to  
428  $50^\circ\text{C}$ ). In this example, a temperature rise of  $25^\circ\text{C}$  can thus be simulated by any of the following  
429 combinations: (a) adding 2% oil to the 40/60pen and testing at  $46^\circ\text{C}$ ; (b) adding 4% oil and testing  
430 at  $43^\circ\text{C}$ ; (c) adding 6% oil and testing at  $39^\circ\text{C}$ ; (d) adding 8% oil and testing at  $35^\circ\text{C}$ ; (e) adding  
431 10% oil and testing at  $31^\circ\text{C}$ .

432

433

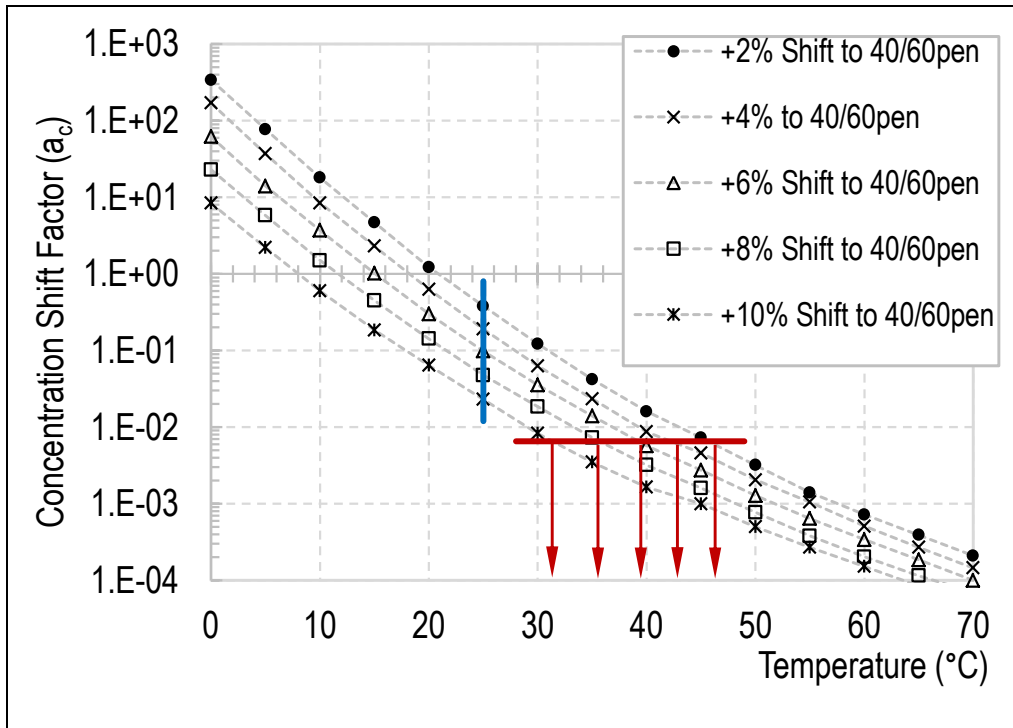


**Fig. 14:** Concentration shift factors for various oil/bitumen blends at various temperatures. Also shown is an example of a line equating shift factor  $a_T$  and  $a_c$  to 0.0065.

434

435 An alternative way of looking at the usefulness of this chart is to fix the required test temperature  
 436 to a predetermined value. For example, the vertical “blue” line shown in Figure 14 represents the  
 437 reference temperature 25°C. At 25°C, the  $a_T$  value for the 40/60pen bitumen would be simply  
 438 equal to 1. Now if we once again make  $a_T = a_c$ , then by adding flux to the 40/60pen, the effect  
 439 becomes equivalent to increasing the test temperature. Thus, adding 2, 4, 6, 8 and 10% flux to the  
 440 40/60pen is equivalent to  $a_c$  values of 0.4, 0.2, 0.1, 0.05 and 0.02 respectively. Accepting the  
 441 argument that  $a_c = a_T$ , the constants  $C_1$  and  $C_2$  for the 40/60pen from Table 1 can be input into

442 equation 13, and the aforementioned  $a_c$  values become equivalent to the following temperature  
443 increments: 2.9°C, 7.0°C, 10.3°C, 13.6°C, 18.5°C respectively.

444 As a further example, referring to Figure 14, if one wishes to rheologically characterize the LVE  
445 properties of a 40/60pen (or an asphalt mix composed of the same binder) at a test temperature of  
446 (25°C + 7°C), one has the option of raising and maintaining the sample temperature at 32°C, or  
447 alternatively blending 4% vegetable oil flux with the bitumen whilst maintaining the sample at the  
448 reference temperature of 25°C.

449

450 **In theory**, once an accurate blending chart is established linking  $a_c$  to  $a_T$  for a particular compatible  
451 bitumen/flux system, high temperature testing can be all carried out at the same reference  
452 temperature. So for example, **by fluxing the bitumen with pre-determined quantities of vegetable**  
453 **oil**, it would be possible to rapidly conduct any number of dynamic modulus tests “representing”  
454 any elevated temperature (e.g. 40, 45, 50, 55°C, etc.) **by simply conditioning all test specimens** at  
455 a constant reference temperature (e.g. 25°C). The savings in time during lengthy temperature  
456 conditioning phase for each test sample (especially if one is conducting tests at many  
457 temperatures), and the number of environmental conditioning cabinets (set at different  
458 temperatures) would be substantial. With the aid of accurate fluxing, all that would be required is  
459 the ability to condition and maintain all test samples to a single reference test temperature.

460

461 Besides the intended reduction in viscosity following fluxing, and as alluded to earlier, as long as  
462 all other rheological characteristics of the base bitumen are maintained (by fluxing only up to a  
463 predetermined limit **whilst** employing a compatible flux), further wider practical implications of

464 fluxing may be envisaged. A hot mix asphalt producer may thus employ fluxing as a means of  
465 producing a range of softer grade bitumens, independently, instantaneously and whenever  
466 required, using a single source of hard bitumen. It would be easy to design an accurate  
467 fluxing/metering unit to be located immediately prior to introducing the binder to the hot aggregate  
468 mix, thus the contractor would only need a single grade of hard base bitumen and potentially a  
469 single hot bitumen storage tank, with potential for cost savings.

470

#### 471 **4. Conclusions:**

472 In summary, this paper proposes and attempts to theoretically justify a workable procedure in  
473 which time-temperature superposition as applied to penetration grade bitumen dynamic shear  
474 rheological (DSR) measurements, may be effectively replaced by time-concentration  
475 superposition. The limited laboratory investigation has demonstrated that it is possible to blend a  
476 small predetermined quantity of a non-volatile vegetable oil flux with a rheologically simple  
477 penetration grade base bitumen, thus affecting the rheological properties of the base bitumen to an  
478 extent equivalent to that obtained when the base bitumen temperature is increased from a reference  
479 test temperature by a fixed and quantifiable amount.

480 To achieve the aforementioned, the methodological steps proposed include; rheological  
481 characterization (preferably by using a DSR) of the base bitumen to produce a master curve at any  
482 selected reference temperature with the accompanying time-temperature shift factors. In the next  
483 stage, rheological data for the blending charts can be easily produced in the laboratory relating the  
484 reduction in any dynamic rheological property (complex viscosity, complex modulus, etc.) of the  
485 base bitumen to the quantity of added flux. In the final stage, by equating the time-temperature

486 shift factors to the time-concentration shift factors, a direct correlation between temperature rise  
487 and added flux content can be achieved.

488

489 Thus at any selected reference temperature, by determining and blending an exact quantity of flux  
490 with the base bitumen, the resultant blend having reduced complex viscosity (or complex shear  
491 modulus) would accurately simulate the rheological characteristics of the base bitumen at a pre-  
492 determined higher test temperature.

493

494 The benefit of the proposed technique becomes particularly relevant when one wishes to conduct  
495 multiple LVE rheological tests (on bitumen or asphalt samples) representing a number of elevated  
496 temperatures, whilst maintaining all samples at a single reference actual test temperature. Thus the  
497 requirement for increasing the actual test temperature to simulate higher environmental  
498 temperature conditions becomes unnecessary. All that is required is a single test temperature to  
499 cover all intermediate or high temperature scenarios.

500

501 Caution must be exercised when fluxing bitumens as there is a tight limit to the amount of flux  
502 that may be added, and furthermore compatibility between the two components must be ensured.

503 The use of Black diagram (complex modulus vs. phase angle) plots was shown to be a useful tool  
504 to assist in identifying flux proportions when blend compatibility becomes suspect.

505

506 Using the proposed methodology hot mix asphalt producers **may** be capable of economically  
507 producing a range of softer bitumen grades according to their needs with the aid of an accurate  
508 flux dosing mechanism and by utilizing a single harder grade base bitumen.

509 **It must be emphasised that the hypothesis, results and analysis presented in this investigation were**  
510 **based on a single sample of penetration grade bitumen fluxed with a single type of vegetable oil.**  
511 **Further laboratory testing must be carried out on a wider range of penetration grade bitumens of**  
512 **different viscosities and chemistries. Extending the concept to polymer modified bitumens is**  
513 **beyond the scope of this investigation.**

514

#### 515 **Acknowledgements**

516 None.

517

#### 518 **Highlights**

- 519 • Time-concentration superposition as an alternative tool to Time-temperature superposition.
- 520 • Bitumens modified with compatible fluxes enable Time-Temperature shift factors to be  
521 effectively interchanged with Time-Concentration shift factors.
- 522 • The rheological properties of fluxed bitumens are simulative of the effects of raising test  
523 temperature.

524

525

526

527

528

529



530 **References:**

531 [AASHTO T 315-12 \(2016\), Determining the Rheological Properties of Asphalt Binder Using a](#)  
532 [Dynamic Shear Rheometer \(DSR\).](#)

533 ASTM D4887/D4887M-11, Standard Practice for Preparation of Viscosity Blends for Hot  
534 Recycled Bituminous Materials.

535 [ASTM D2872-12e1, Standard Test Method for Effect of Heat and Air on a Moving Film of](#)  
536 [Asphalt \(Rolling Thin-Film Oven Test\).](#)

537 [ASTM D6521-13, Standard Practice for Accelerated Aging of Asphalt Binder using a](#)  
538 [Pressurized Aging Vessel \(PAV\).](#)

539 Bailey H.K. & Zoorob S.E., “The use of vegetable oil as a rejuvenator for asphalt mixtures”,  
540 published in 5th Eurasphalt & Eurobitume Congress, 13-15 June 2012 Istanbul. Also published in  
541 The UK Institute of Asphalt Technology Yearbook 2013, ISSN 1479-6341, pp. 70-80.

542 Barabás I. and Todoruț I.A., “Predicting the Temperature Dependent Viscosity of Biodiesel-  
543 Diesel-Bioethanol Blends”, Energy & Fuels 2011, 25, pp. 5767-5774.

544 [Barco-Carrion A.J., Perez-Martinez M., Themeli A., Presti D.L., Marsac P., Pouget S., Hammoum](#)  
545 [F., Chailleux E., Airey G.D., “Evaluation of Bio-Materials Rejuvenating Effect on Binders for](#)  
546 [High Reclaimed Asphalt Content Mixtures”](#), [Materiales de Construcción](#), Vol 67, No 327, 2017.

547 Briant J., Denis J., Parc G., “Rheological Properties of Lubricants”, Institut français du pétrole  
548 publications, 1989 Éditions Technip, Paris, ISBN 2-7108-0564-2.

549 Emri I., Knauss W.G., “Pressure Induced Ageing of Polymers”, Third International Conference on  
550 Numerical Methods for Non-Linear Problems, Dubrovnik, Yugoslavia, September 15-18, 1986.

551 Eurobitume web site, accessed 15 August 2017, [http://www.eurobitume.eu/bitumen/types-](http://www.eurobitume.eu/bitumen/types-bitumen)  
552 bitumen.

553 Erhan S.Z., “Vegetable Oils as Lubricants, Hydraulic Fluids, and Inks”, Chapter 7 in Bailey’s  
554 Industrial Oil and Fat Products, 6th edition, Edited by Shahidi F., 2005 Wiley & Sons, pp. 259-  
555 278.

556 [Ferry J.D., Viscoelastic Properties of Polymers, 3<sup>rd</sup> Edition, John Wiley & Sons, ISBN 0-471-](#)  
557 [04894-1, March 1980.](#)

558 Gawel I.A., Pilat J., Radziszewski P., Niczke L., Krol J. and Sarnowski M., Bitumen Fluxes of  
559 Vegetable Origin”, *Polimery* 2010, 55, nr 1, pp. 55-60.

560 Gedde U.W., Polymer Physics, Springer Science and Business Media, 11 Dec. 2013, ISBN 978-  
561 0-412-62640-1, Section 5.4.

562 Hunter R.N., Self A., Read J., The Shell Bitumen Handbook 6th edition 2015, Appendix 3,  
563 Blending Charts and Formulae, ISBN 978-0-7277-5837-8.

564 [Król J.B., Niczke, L., Kowalski K.J. “Towards Understanding the Polymerization Process in](#)  
565 [Bitumen Bio-Fluxes”, \*Materials\* 2017, 10, 1058.](#)

566 [O’Brien R.D. \(2004\) “Fats and oils-formulating and processing for applications”. 2nd Edition,](#)  
567 [Boca Raton FL, USA: CRC Press; ISBN 0-8493-1599-9, 2004.](#)

568 Rowe G.M. and Sharrock M.J., “Alternative Shift Factor Relationship for Describing the  
569 Temperature Dependency of the Visco-Elastic Behaviour of Asphalt Materials”, Transport  
570 Research Board, Vol. 2207, 2011, pp 125-135.

571 Roy S., Nagendra D., Liechti K.M., “Cohesive-zone modelling of debond growth at adhesively  
572 bonded interfaces in aggressive environments”, International Conference on Fracture (ICF10),  
573 Honolulu USA, Oct. 14, 2001.

574 [Rwei S.P., Lien C.C., “Synthesis and viscoelastic characterization of sulfonated chitosan  
575 solutions”, Colloid Polym Sci, No. 292, pp 785-795, 2014.](#)

576 Schausberger A., Ahrer I.V., “On the time-concentration superposition of the linear viscoelastic  
577 properties of plasticized polystyrene melts using the free volume concept”, Macromol. Chem.  
578 Phys., 196, pp. 2161-2172, 1995.

579 Soleymani H.R., Bahia H.U., Bergan A.T., “Blending Charts Based on the Performance Graded  
580 (PG) Asphalt Binder Specifications”, Transportation Research Record: Journal of the  
581 Transportation Research Board, 1661, pp. 7-14, 1999, Washington D.C.

582 [Tan C.P., Che Man Y.B., Selamat J., and Yusoff M.S.A., Application of Arrhenius Kinetics to  
583 Evaluate Oxidative Stability in Vegetable Oils by Isothermal Differential Scanning Calorimetry,  
584 JAOCS, Vol. 78, no. 11 \(2001\).](#)

585 U.S. DoT, accessed 15 June 2015, Federal Highway Administration, Pavement Recycling  
586 Guidelines for State and Local Governments, Chapter 7, Hot Mix Asphalt Recycling (Materials  
587 and Mix Design), <http://www.fhwa.dot.gov/pavement/recycling/98042/07.cfm>.

588 Yusoff N.I.M., Chailleux E. and Airey G.D., “A Comparative Study of the Influence of Shift  
589 Factors on Master Curve Construction”, *Int. J. Pavement Res. Technol.*, Vol.4 No.6, pp. 324-336,  
590 Nov. 2011.